ELSEVIER

Surface Science 451 (2000) 124–129

surface science

www.elsevier.nl/locate/susc

Time-of-flight techniques for the investigation of kinetic energy distributions of ions and neutrals desorbed by core excitations

R. Weimar [a,*], R. Romberg [a], S.P. Frigo [b], B. Kassühlke [a], P. Feulner [a]

[a] *Physikdepartment E 20, Technische Universität München, D-85747 Garching, Germany*
[b] *Advanced Photon Source, Argonne National Laboratory, 9700 S. Cass Ave., Argonne, IL 60439, USA*

Received 5 August 1999; accepted for publication 2 December 1999

Abstract

We present simple devices operating on the basis of mass spectrometers and time-of-flight techniques for the detection of kinetic energy distributions of neutrals and ions desorbed by photon excitation from adsorbates. We use data on photon stimulated desorption of O^+ and O^0 from chemisorbed monolayers of CO to demonstrate the capabilities of our instruments. Different trends of the kinetic energy distributions as a function of the photon energy are revealed for the two species and explained on the basis of previously obtained results. The future potential of the methods is discussed. © 2000 Elsevier Science B.V. All rights reserved.

Keywords: Carbon monoxide; Desorption induced by electronic transitions (DIET); Ion emission; Photon stimulated desorption (PSD); Ruthenium; Surface photochemistry

1. Introduction

In gas phase experiments on core excitation induced photodissociation, the determination of the kinetic energy (KE) of photoions from their time-of-flight (TOF) in the detector is a common technique which yields valuable information on the microscopic details of the electronically stimulated reaction, in particular if combined with measurements of photoelectrons and decay electrons (see e.g. Ref. [1]). On surfaces, and particularly for strongly coupled chemisorbates on metals, the experimental situation is more difficult, because rapid charge transfer very efficiently shifts intensity from ionic to neutral desorption channels, as well as to recapture (see e.g. Ref. [2]). Apart from exotic multi-hole multi-electron excitations, the escape probability for ions is commonly much smaller than unity for chemisorbates on metals. In the near threshold region, photon stimulated desorption (PSD) of ions can be quenched completely, whereas core excitation-induced desorption of neutrals (molecules and atoms) still persists. Experimental tools are therefore required which yield KE distributions for ions *and* for neutrals, in particular if the cross-over from mainly neutral (for one-electron excitations) to mainly ionic PSD (for multi-electron excitations) is of interest. Because of the small core level excitation cross-sections, the small escape probability particularly for ions, and the limited photon flux that is available under narrow bandwidth excitation conditions, these instruments have to be sufficiently sensitive, for ions as well as for neutrals.

We have designed simple, but sensitive KE detectors for ions and neutrals. After a detailed

* Corresponding author.

PII: S0039-6028(00)00017-0

description of the experimental techniques, we report data on PSD of neutrals and ions from CO/Ru(001)-($\sqrt{3}\times\sqrt{3}$) by O1s excitation. We use this system for a demonstration of the performance of our approach because (i) the CO molecules are well-ordered and bound at identical sites, (ii) the DIET cross-section is maximum for the ($\sqrt{3}\times\sqrt{3}$) coverage [3], and (iii) ample data exist from previous experiments, for PSD of ions [4,5] as well as of neutrals [5].

2. Experiment

The ion data were taken at the PM-5 beamline at BESSY-I, Berlin, in the single bunch modus (SB) of the storage ring, and the KE distributions of neutrals were measured at the BW3 beamline of HASYLAB at DESY in Hamburg. The Ru(001) substrate was cleaned by Ar^+ sputtering, heating in oxygen, and annealing, and the cleanliness was checked by photoelectron spectroscopy. The CO/Ru(001)-($\sqrt{3}\times\sqrt{3}$) layers were prepared by dosing CO in excess, and subsequent heating and annealing under control of thermal desorption spectroscopy. The light was 7° grazing with respect to the surface, with the polarization vector either fully within the surface plane (A_{xy} polarization) or 7° off-normal (A_z). The system base pressure was between 2×10^{-11} mbar (HASYLAB) and 3×10^{-11} mbar (BESSY-I).

KE distributions of desorbing positive ions were measured with the set-up depicted in Fig. 1. It is derived from an electron TOF spectrometer that has previously been used for the investigation of photon induced electron emission in the near threshold region [6]. It consists of a plane, grounded entrance grid of high transparency, a field free drift path the length of which is variable between 150 and 340 mm, and a stack of microchannel plates (MCPs) as ion detector with two grids in front. The sample is located at a distance of 2 mm in front of the entrance grid and positively biased ($300\ \mathrm{V} < U_{\mathrm{sample}} < 1000\ \mathrm{V}$). Ions are desorbed by narrow bandwidth photon pulses of 300 to 500 ps duration at a repetition rate of 208 ns (SB mode of BESSY-I). They are accelerated into the TOF tube, pass through the drift path between the entrance grid and the first grid of the MCP assembly with constant velocity, and are further accelerated by a negative voltage that is applied to the second grid of the MCP assembly. They finally enter the MCP stack which is optimized for minimal skew in time, and the resulting electron pulses are processed with a fast multichannel analyzer (see Ref. [6] for details). The multichannel analyzer processes up to four events per one period of 208 ns. The front side of the first MCP is positively biased with respect to the second grid by 50 V. All potentials are selected in such a way that (i) optimum shapes of the ion TOF spectra are obtained (see below), (ii) fast photo and decay electrons which would yield signals much larger than the ions are prevented from entering the MCP stack, (iii) the ions have sufficiently high kinetic energies for good quantum yields of the MCPs, and (iv) the front side of the first MCP faces a negatively biased environment in order not to lose slow secondary electrons. We obtain spectra with several peaks according to the number of ion species that are desorbed. For O1s excitation of CO/Ru(001), we obtain maxima for O^+, C^+, O^{2+}, and CO^+. From the positions of the trailing edges of the individual peaks on the TOF scale we obtain the masses of the individual ions, and from the shapes of the maxima the KE distributions. Intrinsic KE adds to that acquired by the electrostatic acceleration between the surface and the entrance grid and shortens the flight time of the particles, shifting their maxima to the left on the TOF scale.

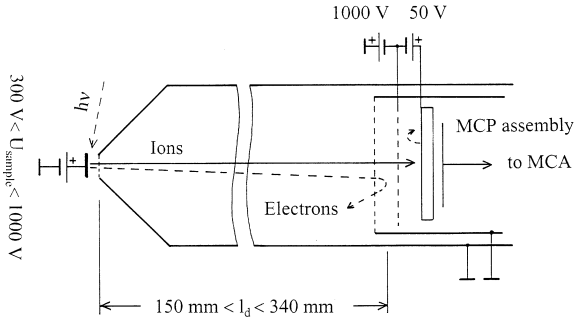

Fig. 1. TOF device for the measurement of kinetic energy distributions of desorbing ions (see text for details).

We note that without further evaluation the

spectra are not unambiguous, because the transit times of the ions are longer than one SB period. This ambiguity is removed by (i) calculations of the ion transit times as a function of their masses and initial KE, and (ii) calibration runs with different potentials and different lengths of the drift path l_d. Two different modes of operation are possible. In the low resolution mode we adjust l_d and U_{sample} in such a way that we obtain all maxima well separated, although not optimally resolved in shape because of the limited space that is available for each peak on the TOF scale between two light pulses. In the high resolution mode we make l_d long and U_{sample} small, warranting a good KE resolution (after transformation from the TOF into the KE domain) for *one selected* species. For $l_d = 340$ mm and $U_{sample} = 300$ V, we obtain $\Delta EK = 0.12$ eV for mass 16 (O^+). To avoid overlapping of the individual peaks which are broader under these conditions compared with the overview modus sketched above, we fine-adjust our potentials in order to separate only one maximum. All the others are shifted together and moved to the edges of the spectrum.

We cannot so far measure negative ions with our device. For valence excitations, cross-sections for DIET of negative ions from chemisorbates are smaller by one to two orders of magnitude than those for DIET of positive ions [7]. We believe that negative ions are not important in our study, because for primary core level excitations their relative amount is probably further decreased by the loss of negative charge upon core hole decay.

The neutral particles are detected with a highly sensitive quadrupole mass spectrometer (QMS) fitted with a liquid helium cooled copper cap over the ionizer (see Fig. 2). The residual gas molecules in the ionizer region are removed by condensation and cryo-trapping onto the inner surfaces of this cap. Two Ti evaporation sources around the ionizer and around the QMS rod assembly deposit an efficiently pumping getter film onto the cold inner surface of the liquid helium cooled containment [8]. In order to obtain KE distributions of the desorbing neutrals, we modulated the ion source of the QMS by applying a skewed square wave potential, which varies between +10 and +120 V with respect to ground, to its continuously

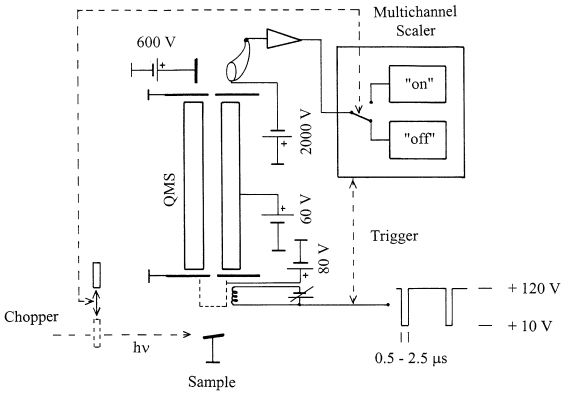

Fig. 2. Block diagram of the experimental arrangement used for the measurement of kinetic energies of desorbing neutral particles (see text for further details; the l-He cryostat and the Ti evaporation sources are not shown).

heated filament. Electron emission and electron impact ionization only occur during the duration of the periodic minimum of this voltage. The KE of the particles is derived from their TOF between ionization and detection with a channeltron. As for the ion detector described above, intrinsic KE shortens the transit time through the mass filter. The electron emission current (0.3 mA for the duration of the pulse), the electron energy (70 eV), the field axis potential of the QMS filter with respect to the ionizer (20 eV), and the duration of the electron pulses (from 500 ns to 2.5 µs) are optimized for maximum sensitivity in combination with best TOF resolution. In particular, the low electron emission current is decisive for a minimal broadening of the TOF distributions by space charge accumulation. To discriminate the background signal due to residual gas, we chop the photon beam at a frequency of about 20 Hz with a duty cycle of 50%, and accumulate the signal from the electron multiplier in different pages of the multichannel scaler for the on/off periods. We then subtract the background signal (i.e. we subtract 'off' from 'on'), and deconvolute the transmission function of our detector from the TOF distributions obtained in the PSD experiment. To obtain the transmission function, we measure TOF distributions of slow particles which have the same mass as those monitored in the PSD experiment. For the calibration of the O^0

spectra of Fig. 4 which have been obtained from chemisorbed $C^{18}O$, we have recorded TOF distributions of *thermally* desorbed water molecules from condensed layers of H_2O on the substrate. Because water sublimates well below room temperature [9], the water molecules are slow compared with the O atoms desorbed by photon excitation, and the transmission function of the analyzer is well resolved. We stress that the transmission function is exclusively governed by the electron optics of the ionizer and its extraction lens. The electric field of the quadrupole mass filter has only azimuthal components, which do not affect the KE component of the particles which is parallel to the axis of the mass filter. For the transformation of the data from the TOF into the KE domain, we use the functional dependence of the TOF on the initial KE which we calculate with the software package Simion. In particular, the experimentally obtained flight time of the slow particles of the calibration runs is reproduced by these calculations with an error of less than the channel width of the multichannel scaler.

Transforming from the TOF into the KE domain, we make energy dependent corrections of the signal amplitudes according to the Jacobian of the transformation (because of the strong post-acceleration, these corrections are very small for the KE distributions of ions). For the neutrals we also correct for the KE dependent ionization probability of the electron impact ionizer, which essentially is a density and not a flux detector. We note that the main disadvantage of our TOF devices is that the exact calibration of the zero point of the KE scale is difficult. Differential KE shifts are much more accurate than the absolute value. Despite this drawback, however, we think that these methods are useful because (i) the acquisition of two-dimensional areas of closely spaced KE = KE($h\nu$) data points as depicted in Fig. 3 for PSD of ions is very time consuming with conventional, low transmission mass spectrometers and energy dispersive analyzers, and (ii) to the best of our knowledge no data exist as yet on the KE of any neutral atomic or molecular species desorbed by narrow bandwidth core excitation.

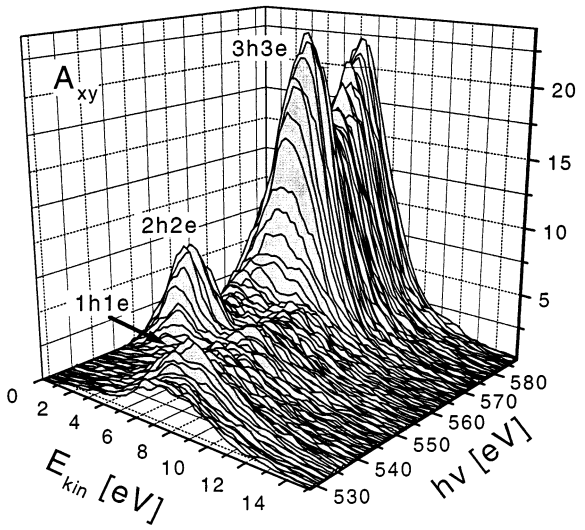

Fig. 3. Pseudo 3D-plot of the kinetic energy distribution of O^+ ions desorbed by O1s excitation from CO/Ru(001)-($\sqrt{3}\times\sqrt{3}$) as a function of the photon energy (A_{xy} light).

3. Results

Fig. 3 shows KE distributions of O^+ ions desorbed by O1s excitations (A_{xy} light). Resonances appear at 533, 550 and 570 eV for this polarization, which have previously been assigned to 1h1e, 2h2e and 3h3e excitations ([O1s]2π, [O1s1π]$2\pi^2$, and [O1s$1\pi^2$]$2\pi^3$, respectively [4]). The assignment of the π-resonance is unambiguous, and that of the 2h2e state has been corroborated by polarization resolved photoabsorption measurements for the isolated molecule [10] and by calculations [11]. For photon energies beyond 570 eV we find a shallow minimum of the O^+ yield followed by a continuous increase due to multiple shake-off states [4]. In the pre-threshold region, the O^+ signal due to valence and C1s excitations is rather small.

Inspecting Fig. 3 we can clearly discriminate different regions of KE. The fastest O^+ ions are observed in the pre-threshold region, for the π-resonance, and for the energy range between the π-resonance and the onset of the multi-electron states. Data obtained in the high resolution mode of our instrument (not shown; because of the limited space available here, we can only present a selection of our data; more details will be pub-

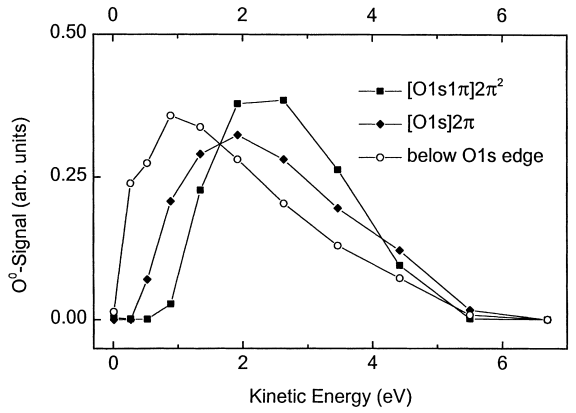

Fig. 4. Kinetic energy distributions of neutral O atoms desorbed from CO/Ru(001)-($\sqrt{3}\times\sqrt{3}$) for excitation (a) below the O1s photoabsorption edge, (b) at the [O1s]2π resonance, and (c) at the [O1s1π]$2\pi^2$ resonance.

lished elsewhere [12]) show that the KE distribution at the π-resonance is bimodal with a second maximum extending to higher KE. The ions with the lowest KE are observed for 2h2e excitations, although the fast channel that predominates for the pre-threshold and the π-resonant regions persists there as well, and is slightly enhanced at the energy position of the 2h2e state. Proceeding to even higher photon energies, we find a fourth KE channel at the 3h3e state, which also exists beyond the threshold for multiple shake-off states. In spectra recorded with A_z light we find identical, well-separated regions of kinetic energy (not shown). The KE values are very similar for the 1h, 2h, and 3h regions to those obtained with A_{xy} light, apart form the fact that no resonances but only thresholds are visible [4,12].

The KE distributions of the neutrally desorbed O atoms show contrasting behavior, Fig. 4. The atoms desorbed in the pre-threshold region by valence and C1s excitations exhibit the lowest KE, those desorbed by π-resonant excitation are faster, and those originating from the 2h2e excitation are fastest. Higher resonances, e.g. the 3h3e state, do not show up in PSD of neutral fragments [5]. (The 1h1e and 2h2e KE data of Fig. 4 have been obtained *after* subtraction of the pre-threshold signal due to valence and C1s excitations from the original TOF data.)

From the above results we can draw the following conclusions. The KE distributions of O atoms behave as expected. Multiply excited states with dissociative asymptotic for the primary core-excited as well as for the multi-hole, multi-electron post-decay states yield the highest KE. (We note that the KE distributions obtained for desorption of neutral CO molecules are much narrower than those for O atoms, particularly for the pre-threshold regime [12].) For ions a contrasting behavior is obtained for the 1h1e region. The KE values are very different for ions and neutrals, and the ion signal is very small. Obviously, completely different reaction channels are monitored. Desorbing O atoms constitute the majority of desorbing fragments, whereas O^+ ions are only a minority, probably due to minority channels in core hole decay like decay satellites, which produce highly repulsive and highly charged final states.

The branching is changed for the 2h regime. (We note that the ion KEs obtained for the resonances and in the shake-off region are very similar, indicating that primary states with similar potential curves and decay behavior are obtained, for either direct population of the antibonding 2π-orbital at the resonance, or by charge transfer screening from the metal in the continuum region.) Here PSD of ions *and* of neutrals is enhanced, and their KE distributions overlap. A common origin is likely for the two species. Particles with higher energy desorb as ions, whereas slower atoms become neutralized. In the high KE resolution mode we find small but reproducible blue-shifts of the O^+ KE across the 2h2e resonance (not shown). Because the primary 2h2e state is repulsive, the O nucleus acquires KE on the potential curve of the core excited state (ultrafast bond breaking, UFD) as well as on the potential curve of the multiply excited valence state after core decay. Preliminary classical calculations indicate that the observed blue shift is *not* a direct result of UFD, but must mainly be due to the evolution after the core hole decay. We hope that a more refined theoretical analysis of our data, which is in progress, will elucidate the dynamics of this interesting system. For the 3h3e region finally charge transfer screening is too slow to neutralize the desorbing particles. PSD of neutrals becomes negligible, and the KE of the ions is further increased.

4. Conclusions

In summary, we have shown that simple TOF devices can supply interesting results on DIET from adsorbates. The performances of our set-ups can be considerably improved in the future, for the ion experiment by using undulator radiation for increased count rates, and for the neutrals by applying an ionizer with better ion optics for increased sensitivity and further decreased broadening of the TOF distributions by space charge accumulation. Particularly for dense two-dimensional ion data sets the TOF approach is unsurpassed.

Acknowledgements

We thank M. Gsell and the staffs of HASYLAB and BESSY for help during the experiments, in particular T. Möller, C. Nowak, A. Kolmakov, C. Hellwig and C. Jung. We are deeply indebted to N. Heckmair, who passed away so untimely. We thank D. Menzel for stimulating discussions and continuous support. Financial support by the Deutsche Forschungsgemeinschaft is gratefully acknowledged (Project SFB 338 C10). S. Frigo acknowledges support by the US Department of Energy, Basic Energy Sciences, Office of Energy Research, under Contract No. W-31-109-ENG-38.

References

[1] N. Saito, F. Heiser, O. Hemmers, K. Wieliczek, J. Viefhaus, U. Becker, Phys. Rev. A 54 (1996) 2004.
[2] P. Feulner, R. Romberg, S. Frigo, R. Weimar, M. Gsell, A. Ogurtsov, D. Menzel, Surf. Sci. 451 (2000) 41.
[3] P. Feulner, S. Auer, T. Müller, A. Puschmann, D. Menzel, in: R.H. Stulen, M.L. Knotek (Eds.), Desorption Induced by Electronic Transitions, DIET-III, Springer, Berlin, 1988, p. 178.
[4] R. Treichler, W. Wurth, E. Riedl, P. Feulner, D. Menzel, Chem. Phys. 153 (1991) 259.
[5] S.P. Frigo, P. Feulner, B. Kassühlke, C. Keller, D. Menzel, Phys. Rev. Lett. 80 (1998) 2813.
[6] P. Feulner, P. Averkamp, B. Kassühlke, Appl. Phys. A 67 (1998) 657.
[7] V.N. Ageev, Progr. Surf. Sci. 47 (1994) 55 and references cited therein.
[8] R. Romberg, S.P. Frigo, A. Ogurtsov, P. Feulner, D. Menzel, Surf. Sci. 451 (2000) 116.
[9] P.A. Thiel, T.E. Madey, Surf. Sci. Rep. 7 (1987) 211.
[10] E. Shigemasa, T. Hayaishi, T. Sasaki, A. Yagishita, Phys. Rev. A 47 (1993) 1824.
[11] H. Ågren, R. Arneberg, Phys. Scr. 30 (1984) 55.
[12] R. Weimar, R. Romberg, P. Feulner, in preparation.